ChemComm

COMMUNICATION

View Article Online
View Journal | View Issue

Cite this: *Chem. Commun.*, 2019, **55**, 6567

Received 3rd April 2019,
Accepted 10th May 2019

DOI: 10.1039/c9cc02596k

rsc.li/chemcomm

A bi-functional redox mediator promoting the ORR and OER in non-aqueous Li–O_2 batteries†

Hao Liu,‡ Mingqiang Liu,‡ Luyi Yang, * Yongli Song, Xingbo Wang, Kai Yang and Feng Pan *

Herein, a bi-functional homogeneous redox mediator is employed to promote the rate capability of Li–O_2 batteries. The addition of this redox mediator not only facilitates the formation of toroid-shaped Li_2O_2 at high current densities, but also significantly reduces the charging over-potential caused by the bulky Li_2O_2.

The demand for providing energy to hybrid energy vehicles has posed new problems: how to improve the specific energy and capacity of the batteries even further.[1,2] The overall capacity of lithium batteries is currently limited by positive electrode materials. As a promising candidate for the next-generation energy storage system, lithium–O_2 batteries have attracted wide attention due to their extremely high theoretical energy density (3505 W h kg^{-1}).[3] Though great progress has been made, there are many problems that need to be solved for further application. Typically, the poor conductivity of the discharge product Li_2O_2 and the sluggish oxygen reduction reaction/evolution reaction (ORR/OER) kinetics lead to low energy efficiencies and poor rate capabilities.[4] One effective strategy is to use catalysts (*e.g.* transition metal oxides,[5,6] noble metals[7,8] polyoxometalates[9] and TiN[10]) at the positive electrode, resulting in accelerated kinetics of the ORR/OER. However, apart from the high costs of noble metals and transition metal oxides, the charge transfer between the catalysts and the electrode materials is not efficient due to a solid–solid interphase. Alternatively, soluble catalysts or redox mediators (RMs) have been extensively studied in recent years due to the fact that a larger effective contact area can be achieved.[11,12] For the OER process, instead of the direct oxidization of Li_2O_2, RMs are first oxidized at a much lower potential. Then the oxidized RMs can chemically oxidize Li_2O_2, leading to a much lower charging over-potential.[13–17] The RMs for the ORR process work in a similar way, where the electrochemically reduced RMs could chemically reduce O_2 to Li_2O_2.[18–20] Most of the current studies focus on the former since unlike the insoluble and insulating Li_2O_2 species, the reduction of soluble O_2 species is diffusion-oriented. Therefore, at low current densities, the ORR normally does not exhibit large over-potentials. However, considering the low solubility of O_2 ($\sim$6.6 mM) in many organic solvents,[21] a depletion of soluble O_2 at the electrode surface can be expected when a relatively high discharging current density is applied.

Herein, a new bi-functional RM is proposed: 1,1′-diheptyl-4,4′-bipyridinium (heptyl viologen) dibromide ($HeptVBr_2$), the molecular structure of which is shown in Fig. S1 (ESI†). Upon adding 5 mM $HeptVBr_2$ into an electrolyte, the rate capability of both the ORR and OER is greatly improved. It is found that as an RM for the ORR, $HeptV^{2+}$ facilitates an accelerated formation of Li_2O_2 in the solution phase whereas Br^- lowers the charging over-potential for the OER process. As a result, the cell exhibits a state-of-the-art discharging current density of 4000 mA g^{-1} (4 mA cm^{-2}) for 1800 mA h g^{-1} in the presence of $HeptVBr_2$. This proposed approach may be applied broadly to develop Li–O_2 batteries with excellent rate capabilities.

Fig. 1 shows the cyclic voltammogram (CV) curves of the ORR and OER with and without the addition of 5 mM $HeptVBr_2$ in an O_2-saturated electrolyte consisting of 0.5 M $LiNO_3$ + 0.5 M bis (trifluoromethane) sulfonimide lithium salt (LiTFSI) in diethylene glycol dimethyl ether (diglyme). In the absence of $HeptVBr_2$, large polarizations are observed for both the ORR and OER, which can be attributed to the relatively electrochemical reaction rates, especially for the insulating Li_2O_2. By contrast, not only the onset potential for the OER with the additive (3.61 V) is much lower compared with the cell without the additive (3.83 V), but also a much higher peak current is obtained with the addition of $HeptVBr_2$. According to the previous literature, after being electrochemically reduced, viologen-based species react with O_2, forming superoxide radicals.[22] Next, in the presence of Li^+, superoxide radicals are found to further react with V^+, forming Li_2O_2.[19] During the ORR process, $HeptV^{2+}$ is first electrochemically reduced to $HeptV^+$, which further chemically reduces O_2 to Li_2O_2:

School of Advanced Materials, Peking University Shenzhen Graduate School, Shenzhen 518055, China. E-mail: panfeng@pkusz.edu.cn, yangly@pkusz.edu.cn

† Electronic supplementary information (ESI) available. See DOI: 10.1039/c9cc02596k

‡ These authors contributed equally to this work.

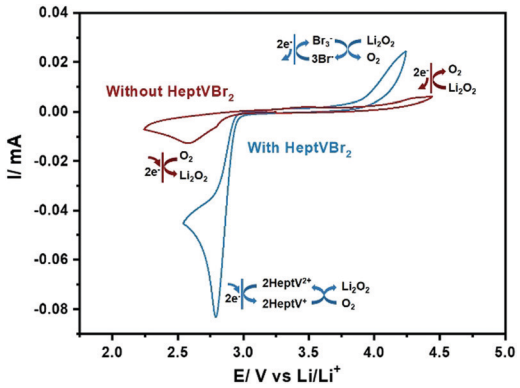

Fig. 1 CV curves and schematic reactions for the ORR and OER with and without the addition of $HeptVBr_2$.

$$HeptV^{2+} + e^- \rightarrow HeptV^+ \quad (1)$$

$$HeptV^+ + O_2 \rightarrow HeptV^{2+} + O_2^- \quad (2)$$

$$2Li^+ + HeptV^+ + O_2^{-\bullet} \rightarrow Li_2O_2 + HeptV^{2+} \quad (3)$$

Since the oxidized $HeptV^{2+}$ can be reduced again, intensified cathodic currents can be obtained due to such a looping effect. Similarly, as for the OER process, Br^- is electrochemically oxidized to Br^{3-}. Then, Br^{3-} chemically oxidizes Li_2O_2 to O_2:[23,24]

$$3Br^- - 2e^- \rightarrow Br_3^- \quad (4)$$

$$Li_2O_2 + Br_3^- \rightarrow O_2 + 2Li^+ + 3Br^- \quad (5)$$

To study the effect of $HeptVBr_2$ on the rate capability, the discharging voltage profiles of different Li–O_2 cells at different current densities are presented in Fig. 2a and b. It can be seen that at a lower current density (1 mA cm^{-2}), two cells exhibit very similar discharging voltage plateaus for 1200 mA h g^{-1}. As the current density increases, a relatively high discharge plateau at approximately 2.30 V for the cell with $HeptVBr_2$ can be obtained even at a current density of 4 mA cm^{-2} which outperforms other currently reported results (see Table S1 for detailed comparisons with other heterogeneous catalysts and homogeneous redox mediators, ESI†), whereas the other cell shows a prominent voltage drop at high current densities. More specifically, the median discharging voltages increase from 2.29 V to 2.44 V at a current density of 2 mA cm^{-2} and from 2.24 V to 2.38 V at a current density of 3 mA cm^{-2}, respectively. The different rate performances can be attributed to the fast electrochemical–chemical (EC–C) reactions in the presence of $HeptVBr_2$ compared with the kinetically sluggish ORR. Moreover, both cells are discharged to failure at a current density of 1 mA cm^{-2}. As shown in Fig. 2c, after the addition of $HeptVBr_2$, the capacity of the Li–O_2 cell was greatly boosted from 2450 mA h g^{-1} to 4200 mA h g^{-1}. Even at a current density of 4 mA cm^{-2}, a capacity of 1800 mA h g^{-1} is obtained after complete discharge (see Fig. S2, ESI†).

To further investigate the effect of $HeptV^{2+}$, HeptV trifluoromethanesulfonate ($HeptV(OTf)_2$) was prepared to exclude the effect of Br^-. First, a scanning electron microscope (SEM) is used to observe the cathodes after discharge. Fig. 3a and b show that without $HeptVBr_2$, the morphology of the discharged cathode is barely changed, indicating the formation of a small and amorphous discharging product on the electrode. By contrast, with the addition of $HeptVBr_2$ and $HeptV(OTf)_2$, toroid-shaped domains can be clearly observed on the O_2 electrode after discharging at such a high current density (shown in Fig. 3c and d). The reduction product presented in Fig. 3b was examined by Raman spectroscopy. As shown in Fig. S3 (ESI†), two characteristic peaks at 240 and 742 cm^{-1} confirm that all the reduction products shown in Fig. 3b–d are Li_2O_2. As previously reported, the toroid-shaped Li_2O_2 is a consequence of solution nucleation/precipitation at a low current density.[25] Additional experiments have been carried out to confirm this result: as shown in Fig. S4 (ESI†), toroid-shaped Li_2O_2 can be observed at the positive electrode after discharging at a low current density without $HeptVBr_2$. Since the cell fails when the cathode is completely passivated by the insulating Li_2O_2 film,[26]

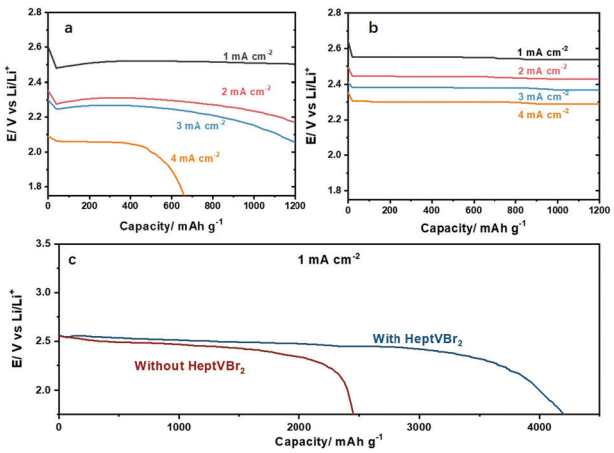

Fig. 2 Voltage profiles of Li–O_2 cells without (a) and with (b) $HeptVBr_2$ at different discharge rates. (c) Voltage profiles of different Li–O_2 cells to 1.75 V at 1 mA cm^{-2}.

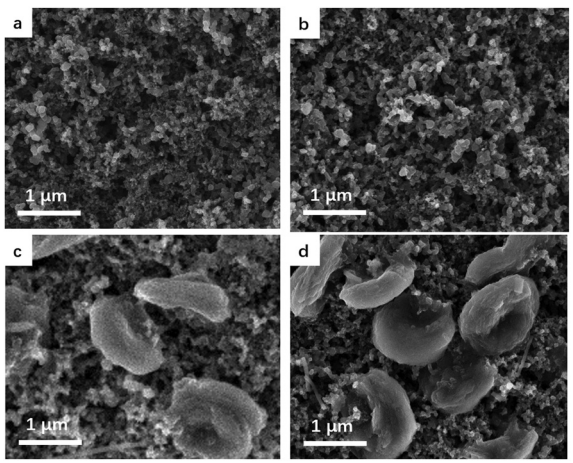

Fig. 3 SEM images of (a) pristine O_2 electrode, and electrodes after discharging (b) without the additive and with (c) $HeptV(OTf)_2$ and (d) $HeptVBr_2$.

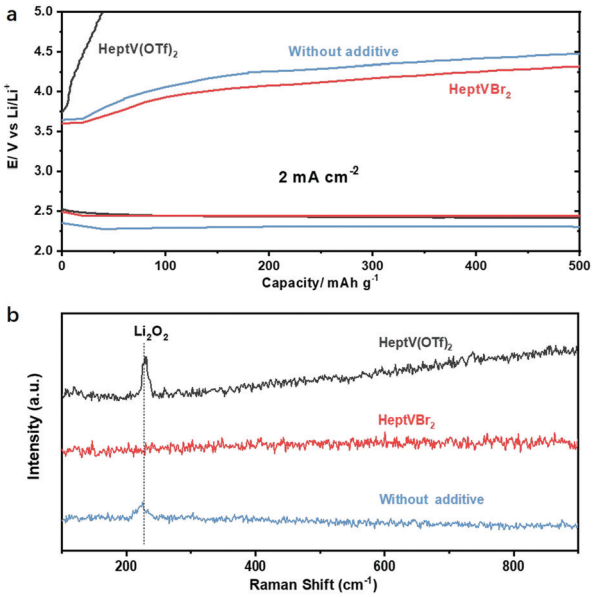

Fig. 4 (a) Voltage profiles of different Li–O_2 cells at a current density of 2 mA cm^{-2}. (b) Raman spectra of different O_2 electrodes after charging.

the toroid-shaped Li_2O_2 domains occupy fewer active sites on the cathode compared with the small and amorphous Li_2O_2 domains so that the passivation of cathode is mitigated, and hence a higher discharge capacity can be obtained. Therefore, for discharging processes, the impact of $HeptVBr_2$ is two-fold: on the one hand, the different rate performances can be attributed to the fast electrochemical–chemical (EC–C) reactions in the presence of $HeptVBr_2$ compared with the kinetically sluggish ORR; on the other hand, the vastly different morphologies of Li_2O_2 could also result in varied discharge capacities.

Although the formation of toroid-shaped Li_2O_2 is beneficial for discharging, it has been reported that such a morphology could lead to even higher charging overpotentials.[25] As shown in Fig. 4a, in the presence of $HeptV(OTf)_2$ and $HeptVBr_2$, discharging voltages are improved compared to the blank group, indicating the promotion effect of $HeptV^{2+}$ on the ORR process. However, the cell with $HeptV(OTf)_2$ can be barely charged. This result suggests that without an OER mediator, a large toroid-shaped Li_2O_2 domain is much more difficult to electrochemically oxidize compared to amorphous Li_2O_2 of much smaller sizes, which may be attributed to the insulating properties of Li_2O_2. By contrast, upon adding $HeptVBr_2$, a much lower charging potential is achieved, indicating that Br^- successfully promotes the OER process and lowers the overpotential as predicted. This conclusion is also supported by the Raman spectra (shown in Fig. 4b) of the positive electrodes in different cells after charging: in the presence of $HeptV(OTf)_2$, a large amount of Li_2O_2 can be observed on the charged electrode, whereas for the cells with $HeptVBr_2$, no Li_2O_2 residue can be detected. To further demonstrate the effect of $HeptVBr_2$ on the OER process, voltage curves at various charging current densities are presented in Fig. S5 (ESI†). It can be seen that although $HeptV^{2+}$ promotes the formation of large crystalline Li_2O_2 domains on the O_2-electrode, the charging over-potential is greatly

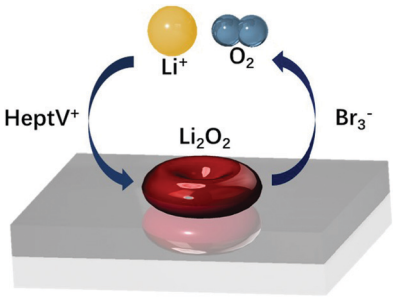

Scheme 1 Schematic illustration of the effect of $HeptVBr_2$ on a Li–O_2 battery.

lowered owing to the presence of Br^-. For instance, at a current density of 2 mA cm^{-2}, the median charging voltage is reduced from 4.29 V to 4.16 V. In addition, the cycling performances for different Li–O_2 cells are also tested (see Fig. S6, ESI†). The result shows that under 2 mA cm^{-2}, the cell with $HeptVBr_2$ still exhibit low over-potentials after 50 cycles, indicating the excellent cycling stability of $HeptVBr_2$.

In this work, we have used $HeptVBr_2$ as a bi-functional homogeneous redox mediator in lithium–oxygen batteries. As demonstrated in Scheme 1, the cation and anion in $HeptVBr_2$ have worked synergistically in order to achieve high-current-density discharging and charging for Li–O_2 batteries. On the one hand, $HeptV^+$ facilitates a promoted ORR process by forming toroid-shaped Li_2O_2 in the solution phase; on the other hand, Br_3^- could chemically breakdown the micron-sized Li_2O_2, which is found to be very difficult to electrochemically oxidize. By introducing a bi-functional redox mediator, this work proposes a new perspective on designing optimal systems for Li–O_2 batteries.

Conflicts of interest

There are no conflicts to declare.

Notes and references

1 J. Lu, Z. Chen, F. Pan, Y. Cui and K. Amine, *Electrochemical Energy Reviews*, 2018, **1**, 35–53.
2 J. Lu, Z. Chen, Z. Ma, F. Pan, L. A. Curtiss and K. Amine, *Nat. Nanotechnol.*, 2016, **11**, 1031–1038.
3 A. Hu, J. Long, C. Shu, R. Liang and J. Li, *ACS Appl. Mater. Interfaces*, 2018, **10**, 34077–34086.
4 N. Feng, P. He and H. Zhou, *Adv. Energy Mater.*, 2016, **6**, 1–24.
5 S. Li, J. Xu, Z. Ma, S. Zhang, X. Wen, X. Yu, J. Yang, Z. F. Ma and X. Yuan, *Chem. Commun.*, 2017, **53**, 8164–8167.
6 S. Tong, M. Zheng, Y. Lu, Z. Lin, J. Li, X. Zhang, Y. Shi, P. He and H. Zhou, *J. Mater. Chem. A*, 2015, **3**, 16177–16182.
7 S. Ma, Y. Wu, J. Wang, Y. Zhang, Y. Zhang, X. Yan, Y. Wei, P. Liu, J. Wang, K. Jiang, S. Fan, Y. Xu and Z. Peng, *Nano Lett.*, 2015, **15**, 8084–8090.
8 V. R. Chitturi, M. Ara, W. Fawaz, K. Y. S. Ng and L. M. R. Arava, *ACS Catal.*, 2016, **6**, 7088–7097.
9 T. Homewood, J. T. Frith, J. P. Vivek, N. Casañ-Pastor, D. Tonti, J. R. Owen and N. Garcia-Araez, *Chem. Commun.*, 2018, **54**, 9599–9602.
10 F. Li, R. Ohnishi, Y. Yamada, J. Kubota, K. Domen, A. Yamada and H. Zhou, *Chem. Commun.*, 2013, **49**, 1175–1177.
11 H.-D. Lim, B. Lee, Y. Zheng, J. Hong, J. Kim, H. Gwon, Y. Ko, M. Lee, K. Cho and K. Kang, *Nat. Energy*, 2016, **1**, 16066.
12 J. B. Park, S. H. Lee, H. G. Jung, D. Aurbach and Y. K. Sun, *Adv. Mater.*, 2018, **30**, 1–13.

13 Y. Chen, S. A. Freunberger, Z. Peng, O. Fontaine and P. G. Bruce, *Nat. Chem.*, 2013, **5**, 489–494.
14 H. D. Lim, H. Song, J. Kim, H. Gwon, Y. Bae, K. Y. Park, J. Hong, H. Kim, T. Kim, Y. H. Kim, X. Leprõ, R. Ovalle-Robles, R. H. Baughman and K. Kang, *Angew. Chem., Int. Ed.*, 2014, **53**, 3926–3931.
15 M. Yu, X. Ren, L. Ma and Y. Wu, *Nat. Commun.*, 2014, **5**, 5111.
16 K. P. C. Yao, J. T. Frith, S. Y. Sayed, F. Bardé, J. R. Owen, Y. Shao-Horn and N. Garcia-Araez, *J. Phys. Chem. C*, 2016, **120**, 16290–16297.
17 S. H. Lee, W. J. Kwak and Y. K. Sun, *J. Mater. Chem. A*, 2017, **5**, 15512–15516.
18 D. Sun, Y. Shen, W. Zhang, L. Yu, Z. Yi, W. Yin, D. Wang, Y. Huang, J. Wang, D. Wang and J. B. Goodenough, *J. Am. Chem. Soc.*, 2014, **136**, 8941–8946.
19 L. Yang, J. T. Frith, N. Garcia-Araez and J. R. Owen, *Chem. Commun.*, 2015, **51**, 1705–1708.
20 M. J. Lacey, J. T. Frith and J. R. Owen, *Electrochem. Commun.*, 2013, **26**, 74–76.
21 B. J. Bergner, A. Schürmann, K. Peppler, A. Garsuch and J. Janek, *J. Am. Chem. Soc.*, 2014, **136**, 15054–15064.
22 E. J. Nanni, C. T. Angelis, J. Dickson and D. T. Sawyer, *J. Am. Chem. Soc.*, 1981, **740**, 4268–4270.
23 W. J. Kwak, D. Hirshberg, D. Sharon, M. Afri, A. A. Frimer, H. G. Jung, D. Aurbach and Y. K. Sun, *Energy Environ. Sci.*, 2016, **9**, 2334–2345.
24 Z. Liang and Y. Lu, *J. Am. Chem. Soc.*, 2016, **138**, 7574–7583.
25 B. D. Adams, C. Radtke, R. Black, M. L. Trudeau, K. Zaghib and L. F. Nazar, *Energy Environ. Sci.*, 2013, **6**, 1772–1778.
26 L. Johnson, C. Li, Z. Liu, Y. Chen, S. A. Freunberger, P. C. Ashok, B. B. Praveen, K. Dholakia, J. M. Tarascon and P. G. Bruce, *Nat. Chem.*, 2014, **6**, 1091–1099.

